Non biogenic source is an important but overlooked contributor to aerosol isoprene-derived organosulfates during winter in northern China

Ting Yang[1], Yu Xu[1,2]*, Yu-Chen Wang[3], Yi-Jia Ma[1], Hong-Wei Xiao[1,2], Hao Xiao[1,2], Hua-Yun Xiao[1,2]

[1]School of Agriculture and Biology, Shanghai Jiao Tong University, Shanghai 200240, China

[2]Shanghai Yangtze River Delta Eco-Environmental Change and Management Observation and Research Station, Ministry of Science and Technology, Ministry of Education, Shanghai 200240, China

[3]Division of Environment and Sustainability, Hong Kong University of Science and Technology, Hong Kong SAR 00000, China

*Corresponding authors

Yu Xu

E-mail: xuyu360@sjtu.edu.cn

25 **Table of Contents**

26 Text S1–S3

40
41
42

43

44

S1. Classification of Organosulfates

Organosulfates (OSs) were identified using an UPLC-ESI-QToFMS (Waters, USA) in negative (−) ion mode (Wang et al. 2021a; Yang et al. 2023). The obtained data were processed with a MassLynx v4.1 software to obtain the m/z ratios, formulas, retention times, and peak areas of identified OSs. A mass spectral library was built using the compound database function; moreover, the identified compounds can be expressed as $C_cH_hO_oN_nS_s$ with a mass tolerance of ±10 ppm (where c, h, o, n, and s represent the number of carbon, hydrogen, oxygen, nitrogen, and sulfur atoms, respectively). Compounds with oxygen atoms equal to or greater than $4n_S + 3n_N$ (i.e., $n_O/(4n_S + 3n_N) \geq 1$) were tentatively classified as OSs (Cai et al. 2020). The assignments of most OSs were further conducted based on their loss of the sulfur-containing fragment ions (e.g., m/z 80, 81, and 96) by MS/MS analysis (Hettiyadura et al. 2015), which was detailed in our recent publication (Yang et al. 2023). The Double Bond Equivalent value (DBE), indicating the number of rings and double bonds in an organic molecule, can be calculated using the following equation (Han et al. 2023).

$$DBE = 1 + n_C - n_H/2 + n_N/2 \qquad (1)$$

where n_N, n_H, and n_C indicate the numbers of N, H, and C atoms in a molecular formula, respectively.

All potential OSs were further classified into five categories according to their carbon number (n_C), nitrogen number (n_N), oxygen number (n_O), and unsaturation degree indexed by DBE, including isoprene-derived (OS_i), monoterpene-derived

67   (OS_m), C_2–C_3 OSs, aromatic OSs and aliphatic OSs (Yang et al. 2023). The list of OS_i

68   was obtained through the following method: (1) molecules with $n_C = 4$ and 5 were

69   selected; (2) C_4 OSs with DBE range of 1–2, $n_O \leq 6$, and $n_H \geq 6$ and C_5 OSs with DBE

70   range of 0–2, $n_O \leq 7$, and $n_H \geq 8$. The detailed workflow was provided by Yang et al.

71   (2023). It should be noted that $C_7H_9O_7S^-$ was classified as OS_i based on a previous

72   study by Nozière et al. (2010b).

73   According to previous laboratory studies, most of OS_m contain 10 carbon atoms,

74   with effective oxygen atoms ($n_{Oeff} = n_O - 2n_N$) exceeding 4, and $2 \leq DBE \leq 4$ (Guo et

75   al. 2022; Ehn et al. 2012; Yan et al. 2016; Jokinen et al. 2014; Boyd et al. 2015;

76   Berndt et al. 2016; Berndt et al. 2018). Additionally, $C_9H_{15}O_6S^-$, $C_7H_{11}O_7S^-$,

77    $C_9H_{14}NO_8S^-$, $C_7H_{11}O_6S^-$, and $C_8H_{13}O_7S^-$ were classified into the OS_m category based

78   on previous studies (Yassine et al. 2012; Nozière et al. 2010a; Wang et al. 2017b;

79   Surratt et al. 2008). Furthermore, a correlation analysis was conducted between the

80   selected OSs and representative OS_m (e.g., $C_{10}H_{17}O_5S^-$) (Bryant et al. 2021).

81   Accordingly, if a significant correlation ($r > 0.6$ and $P < 0.01$) was found between

82   them, the corresponding OS compound was subsequently classified as OS_m.

83   We further classified the remaining OSs based on their DBE values, aromaticity

84   equivalent (X_C), $n_{O\text{-eff}}$ and n_N. The aromaticity equivalent (X_c) describes potential

85   monocyclic and polycyclic aromatic compounds. It has been suggested that OSs with

86   DBE ≥ 2 and aromaticity equivalent (X_C) ≥ 2.5 can be classified as aromatic OSs

87   (Jiang et al. 2022; Xie et al. 2021; Xie et al. 2020; Ma et al. 2022). The X_C can be

88   calculated as the following equation (Yassine et al. 2014).

89          $X_C = [3(DBE - (f_m n_O - f_n n_S)) - 2] / [DBE - (f_m n_O - f_n n_S)]$ (2)

90   where the symbols f_n and f_m correspond to the fractions of S and O atoms involved in

91   the π-bond structure of the compound, respectively (Yassine et al. 2014). The negative

92   ion mode exhibits a preferential detection capability for compounds such as

93   carboxylic acids and esters (Ye et al. 2021). Thus, the calculation for Xc of

94   organosulfates can be simplified as the following equation (Ye et al. 2021).

95          $X_C = [3(DBE - 0.5(n_O - 4)) - 2] / [DBE - 0.5(n_O - 4)])$ (3)

96   Nonetheless, previous studies have suggested that a DBE value of 2 for OS_m

97   species can be formed via the oxidation of monoterpene by $NO_3\bullet$ or $\bullet OH$ (Yan et al.

98   2016; Ehn et al. 2014; Trostl et al. 2016). Clearly, it is difficult to completely

99   distinguish aromatic OSs from OS_m based on DBE values. Hence, aromatic OSs with

100   a DBE value of 2 were further screened according to correlation analysis between

101   unidentified aromatic OSs and identified aromatic OSs and OS_m (Yang et al. 2023).

102   The acceptance threshold for the above screening was $r > 0.6$ and $P < 0.01$ (Yang et al.

103   2023).

104   The observed OSs with a DBE < 2, such as alkanes and some other unsaturated

105   compounds, were classified as aliphatic OSs (Xie et al. 2020; Tao et al. 2014).

106   Recently, some aliphatic oxygenated organic molecules were found to have a DBE

107   value of 2 (Wang et al. 2021b). Thus, a correlation analysis was conducted between

108   OSs with DBE = 2 and identified aliphatic species. If a significant correlation ($r > 0.6$

109   and $P < 0.01$) was found between them, the corresponding OS compound was

110   assigned to aliphatic OSs. Additionally, both aliphatic and aromatic OSs were

111   classified as anthropogenic OSs (OS_a) (Riva et al. 2016; Riva et al. 2015).

112

113   **S2. Quantification of OSs**

114   The accurate quantification of OSs is difficult owing to a lack of authentic

115   standards. Consequently, the majority of the identified OSs were quantified using

116   surrogate standards.(Hettiyadura et al. 2019b; Bryant et al. 2021; Wang et al. 2018;

117   Ding et al. 2022a) The surrogate standards utilized in this study were as follows.

118   Glycolic acid sulfate (GAS, $C_2H_3O_6S^-$), lactic acid sulfate (LAS, $C_3H_5O_6^-$),

119   limonaketone sulfate ($C_9H_{15}O_6S^-$), and α-pinene sulfate ($C_{10}H_{17}O_5S^-$) were self

120   synthesized according to previous studies (Olson et al. 2011; Wang et al. 2017a).

121   Methyl sulfate ($CH_3O_4S^-$, 99%, Macklin), potassium phenyl sulfate ($C_6H_5O_4S^-$, 98%,

122   Tokyo Chemical Industry), and sodium octyl sulfate ($C_8H_{17}O_4S^-$, 95%, Sigma-

123   Aldrich) are commercial standards (Olson et al. 2011; Huang et al. 2018b; Wang et al.

124   2018; Wang et al. 2020). Our previous studies have validated the reliability of these

125   surrogates (Wang et al. 2021a; Yang et al. 2023). In this study, 111 OS were quantified

126   using the aforementioned surrogate standards. More details of the methods were

127   described in our previous studies (Yang et al. 2023). The recoveries for these OS

128   standards ranged from 84% to 94%. Further information on the data quality control

129   can be referred to our recent work (Yang et al. 2023). It is crucial to highlight that the

130   OS species quantified in this study should not be interpreted as an exact measurement

131   of OS compounds. Instead, this method represents the optimal approach in the

132   absence of authentic OS standards (Yang et al. 2023; Huang et al. 2023).

133

134   **S3. Estimating of Isoprene Emission Rate**

135   The isoprene emission rate (I) can be calculated using the following equation

136   (Guenther et al. 1993).

137 $$I = Is \times C_L \times C_T \qquad (4)$$

138   where the Is value is the constant at 30°C leaf temperature and 1000 μmol m^{-2} s^{-1}

139   photosynthetically active radiation (PAR). C_L and C_T denote the factors that influence

140   light and temperature, respectively. C_L and C_T can be simply estimated as:

141 $$C_L = \frac{\alpha\, C_{L1} L}{\sqrt{\alpha^2 L^2 + I}} \qquad (5)$$

142

143 $$C_T = \frac{\exp\frac{C_{T1}(T - T_S)}{R T_S T}}{1 + \exp\frac{C_{T2}(T - T_M)}{R T_S T}} \qquad (6)$$

144

145   where C_{T2} = 230000 J mol^{-1}, T_M = 314 K, R = 8.314 J K^{-1} mol^{-1}, α = 0.0027, T_S =

146   303 K, C_{L1} = 1.066, and C_{T1} = 95000 J mol^{-1}. Furthermore, T is leaf temperature (K),

147   and L denotes photosynthetically active radiation (PAR) in μmol m^{-2} s^{-1} (Guenther et

148   al. 1993). Data on daily mean temperature and solar radiation during the sampling

149   periods were downloaded from the National Meteorological Science Data Center

150   (https://data.cma.cn/). PAR was calculated by solar radiation multiplying photon flux

151   efficacy of 1.86 μmol J^{-1} (Ding et al. 2016). The value of $C_L \times C_T$ was employed as an

152   indicator for estimating isoprene emission (Ding et al. 2016; Guenther et al. 1993).

153

154 **Table S1.** The mean values (± SD) of the major parameters observed in different
155 cities.

	Southern cities		Northern cities	
	GZ	KM	TY	XA
T (℃)	15.9 ± 3.25	9.63 ± 2.52	-2.56 ± 2.14	1.69 ± 2.24
RH (%)	62.04 ± 21.39	68.25 ± 7.73	42.74 ± 8.78	49.27 ± 17.47
Wind speed (m/s)	3.27 ± 2.07	4.17 ± 1.11	2.44 ± 1.07	6.33 ± 3.36
NO_2 ($\mu g\ m^{-3}$)	71.07 ± 26.89	44.01 ± 16.15	61.11 ± 33.72	79.02 ± 26.17
O_3 ($\mu g\ m^{-3}$)	34.62 ± 22.76	37.55 ± 16.19	30.07 ± 22.84	24.67 ± 13.35
O_x ($\mu g\ m^{-3}$)	105.69 ± 40.9	81.55 ± 20.2	91.19 ± 15.42	103.69 ± 17.13
$C_L \times C_T$	0.16 ± 0.07	0.07 ± 0.03	0.01 ± 0.00	0.02 ± 0.01
SO_2 ($\mu g\ m^{-3}$)	15.87 ± 6.29	18.45 ± 5.34	60.36 ± 40.28	31.73 ± 12.13
ALW ($\mu g\ m^{-3}$)	19.62 ± 25.35	8.18 ± 6.42	21.18 ± 21.21	51.63 ± 81.74
pH	2.65 ± 0.76	4.06 ± 1.61	5.99 ± 0.92	5.13 ± 0.9
NO_3^- ($\mu g\ m^{-3}$)	6.43 ± 3.53	4.83 ± 3.80	14.95 ± 14.27	40.56 ± 31.79
SO_4^{2-} ($\mu g\ m^{-3}$)	8.96 ± 6.11	8.09 ± 4.53	14.12 ± 13.66	21.58 ± 17.3
Ca^{2+} ($\mu g\ m^{-3}$)	1.01 ± 0.51	2.91 ± 1.07	6.09 ± 1.72	6.69 ± 5.72
Mg^{2+} ($\mu g\ m^{-3}$)	0.05 ± 0.02	0.08 ± 0.03	0.34 ± 0.13	0.36 ± 0.36
$Nss-K^+$ ($\mu g\ m^{-3}$)	0.76 ± 0.59	0.53 ± 0.36	1.20 ± 0.98	2.64 ± 1.99
Na^+ ($\mu g\ m^{-3}$)	0.17 ± 0.11	0.08 ± 0.07	1.69 ± 0.85	1.59 ± 2.36
NH_4^+ ($\mu g\ m^{-3}$)	4.88 ± 2.41	3.78 ± 2.67	12.11 ± 11.66	20.58 ± 17.78
$Nss-Cl^-$ ($\mu g\ m^{-3}$)	0.46 ± 0.43	0.74 ± 0.36	6.39 ± 5.55	5.90 ± 3.80
$PM_{2.5}$ ($\mu g\ m^{-3}$)	56.41 ± 33.06	47.62 ± 30.50	81.02 ± 65.20	115.33 ± 88.85
Total OS_i ($ng\ m^{-3}$)	86.65 ± 60.25	61.12 ± 37.75	170.69 ± 68.75	260.32 ± 71.13
Total OS_m ($ng\ m^{-3}$)	57.81 ± 40.77	58.9 ± 29.70	22.34 ± 7.71	40.09 ± 12.31
Total aromatic-OSs ($ng\ m^{-3}$)	10.31 ± 4.64	7.81 ± 2.25	27.10 ± 17.30	34.75 ± 8.91
Total aliphatic-OSs ($ng\ m^{-3}$)	8.23 ± 3.77	10.41 ± 5.33	14.13 ± 7.91	19.46 ± 8.11
Total C_2-C_3 OSs ($ng\ m^{-3}$)	25.22 ± 15.09	28.55 ± 16.4	13.43 ± 2.34	25.81 ± 10.76

156

157 **Table S2.** The mean mass concentrations (± SD) of identified OS_i, OS_m, and C_2-C_3
158 OSs in $PM_{2.5}$ collected in different cities.

Formula [M-H]⁻	MW (Da)	Southern cities		Northern cities	
		GZ (ng m⁻³)	KM (ng m⁻³)	TY (ng m⁻³)	XA (ng m⁻³)
OS_i					
$C_4H_7O_5S^-$	167.0014	2.7 ± 1.53	2.77 ± 1.71	3.07 ± 0.72	4.74 ± 1.72
$C_4H_6O_5S^-$	165.9936	7.86 ± 4.70	5.97 ± 4.78	29.54± 19.77	23.40 ± 13.74
$C_5H_9O_6S^-$	197.0120	15.94 ± 10.59	11.82 ± 8.42	75.92 ± 46.15	71.09 ± 24.18
$C_4H_7O_7S^-$	198.9912	12.63 ± 10.16	10.38 ± 9.11	10.42 ± 8.97	13.50 ± 3.81
$C_5H_{11}O_6S^-$	199.0276	1.69 ± 1.32	2.04 ± 1.52	2.43 ± 0.85	1.60 ± 0.48
$C_5H_7O_7S^-$	210.9912	6.03 ± 8.30	3.74 ± 2.51	7.65 ± 3.92	10.93 ± 6.24
$C_5H_9O_7S^-$	213.0069	10.07 ± 8.88	6.21 ± 4.34	24.49 ±12.27	104.72 ± 44.75
$C_5H_{11}O_7S^-$	215.0225	3.22 ± 3.36	2.83 ± 1.76	0.73 ± 0.19	1.93 ± 0.62
$C_7H_9O_7S^-$	237.0069	4.74 ± 3.69	1.56 ± 1.27	1.57 ± 0.96	3.35 ± 1.40
$C_5H_8NO_{10}S^-$	273.9869	0.25 ± 0.04	0.29 ± 0.05	0.32 ± 0.07	0.29 ± 0.12
$C_5H_7O_8S^-$	226.9862	10.18 ± 7.12	3.80 ± 2.90	2.25 ± 1.72	5.33 ± 3.26
$C_4H_8NO_7S^-$	243.9763	0.79 ± 0.35	0.74 ± 0.40	1.34 ± 0.53	3.91 ± 1.97
$C_4H_7O_8S^-$	214.9862	0.87 ± 0.41	1.76 ± 1.63	3.62 ± 3.96	1.28 ± 0.78
$C_4H_5O_7S^-$	196.9756	2.40 ± 1.28	1.58 ± 0.70	1.33 ± 0.44	2.36 ± 1.90
$C_4H_6NO_9S^-$	243.9763	0.28 ± 0.06	0.28 ± 0.04	0.24 ± 0.04	0.27 ± 0.06
$C_5H_9O_8S^-$	229.0018	3.07 ± 1.90	3.71 ± 2.49	3.62 ± 2.46	6.86 ± 2.70
$C_5H_{10}NO_9S^-$	260.0076	0.18 ± 0.00	0.23 ± 0.03	0.19 ± 0.01	0.18 ± 0.00
$C_5H_8NO_7S^-$	226.0021	3.74 ± 2.81	1.41 ± 1.00	1.98 ± 1.43	4.59 ± 2.62
OS_m					
$C_7H_{11}O_6S^-$	223.0276	9.51 ± 6.01	6.48 ± 4.59	7.07 ± 3.40	7.67 ± 2.80
$C_7H_{11}O_7S^-$	239.0225	10.23 ± 9.22	5.65 ± 4.62	4.49 ± 2.18	6.68 ± 2.86
$C_9H_{15}O_6S^-$	251.0589	0.23 ± 0.06	0.68 ± 0.24	0.25 ± 0.05	0.41 ± 0.13
$C_8H_{13}O_7S^-$	253.0382	2.05 ± 1.65	0.51 ± 0.13	2.59 ± 1.96	2.56 ± 0.81
$C_{10}H_{15}O_7S^-$	279.0538	8.23 ± 8.25	3.96 ± 3.05	1.87 ± 0.52	3.54 ± 1.88
$C_{10}H_{16}NO_7S^-$	294.0647	18.26 ± 14.43	15.88 ± 11.68	2.62 ± 0.82	6.81 ± 3.17
$C_9H_{14}NO_8S^-$	296.0440	4.58 ± 2.19	20.15 ± 8.81	1.62 ± 0.80	8.92 ± 3.59
$C_{10}H_{16}NO_{10}S^-$	342.0495	1.18 ± 0.52	3.50 ± 2.03	0.71 ± 0.37	1.73 ± 1.67
$C_{10}H_{15}O_5S^-$	247.0640	2.45 ± 2.54	0.58 ± 0.37	0.24 ± 0.02	0.55 ± 0.17
$C_{10}H_{15}O_6S^-$	263.0589	0.26 ± 0.09	0.46 ± 0.17	0.16 ± 0.03	0.37 ± 0.09
$C_{10}H_{17}O_6S^-$	265.0746	0.11 ± 0.01	0.15 ± 0.02	0.11 ± 0.02	0.11 ± 0.01
$C_{10}H_{17}O_8S^-$	297.0644	0.17 ± 0.08	0.19 ± 0.04	0.16 ± 0.04	0.22 ± 0.08
$C_{10}H_{15}O_8S^-$	295.0488	0.13 ± 0.04	0.18 ± 0.04	0.10 ± 0.01	0.12 ± 0.02
$C_{10}H_{17}NO_9S^-$	326.0546	0.10 ± 0.00	0.13 ± 0.02	0.13 ± 0.02	0.11 ± 0.01
$C_9H_{11}O_8S^-$	279.0175	0.23 ± 0.09	0.28 ± 0.07	0.12 ± 0.01	0.17 ± 0.04
C_2-C_3 OSs					
$C_3H_5O_4S^-$	136.9909	1.92 ± 0.64	2.03 ± 0.51	2.52 ± 0.61	3.16 ± 1.04
$C_2H_3O_5S^-$	138.9701	1.39 ± 0.28	1.53 ± 0.26	1.16 ± 0.08	1.16 ± 0.14
$C_3H_5O_5S^-$	152.9858	5.07 ± 2.89	4.12 ± 1.43	2.82 ± 0.55	4.72 ± 1.73
$C_2H_3O_6S^-$	154.9650	8.45 ± 5.52	9.8 ± 6.65	2.25 ± 0.35	5.36 ± 1.94
$C_3H_7O_5S^-$	155.0014	2.31 ± 0.99	3.84 ± 1.81	2.77 ± 1.61	5.47 ± 4.61
$C_3H_5O_6S^-$	168.9807	6.07 ± 5.22	7.24 ± 6.38	1.91 ± 0.69	5.95 ± 2.49

159

160 **Table S3.** The mean mass concentrations (± SD) of identified anthropogenic OSs in
161 PM$_{2.5}$ collected in different cities.

Formula[M-H]$^-$	MW(Da)	Southern cities		Northern cities	
		GZ (ng m^{-3})	KM (ng m^{-3})	TY (ng m^{-3})	XA (ng m^{-3})
Aliphatic OSs					
C$_{12}$H$_{21}$O$_7$S$^-$	309.1008	0.07 ± 0.04	0.04 ± 0.03	0.04 ± 0.04	0.05 ± 0.05
C$_8$H$_{17}$O$_4$S$^-$	210.0926	0.07 ± 0.05	0.45 ± 0.36	0.49 ± 0.21	0.49 ± 0.16
C$_{14}$H$_{29}$O$_5$S$^-$	309.1736	0.15 ± 0.11	0.21 ± 0.07	0.53 ± 0.55	0.46 ± 0.43
C$_7$H$_{15}$O$_4$S$^-$	195.0691	0.12 ± 0.24	0.25 ± 0.18	1.18 ± 0.56	0.87 ± 0.41
C$_7$H$_{15}$O$_5$S$^-$	211.064	0.05 ± 0.04	0.06 ± 0.03	0.06 ± 0.02	0.15 ± 0.10
C$_9$H$_{19}$O$_4$S$^-$	223.1004	0.26 ± 0.11	0.67 ± 0.65	0.90 ± 0.57	1.2 6± 0.74
C$_{10}$H$_{21}$O$_4$S$^-$	237.1161	0.27 ± 0.11	0.44 ± 0.90	0.82 ± 0.34	1.01 ± 0.97
C$_7$H$_{13}$O$_5$S$^-$	209.0484	0.20 ± 0.08	0.16 ± 0.09	0.36 ± 0.10	0.67 ± 0.13
C$_9$H$_{17}$O$_5$S$^-$	237.0797	0.09 ± 0.09	0.09 ± 0.04	0.56 ± 0.26	0.46 ± 0.26
C$_{10}$H$_{19}$O$_5$S$^-$	251.0953	0.82 ± 0.42	0.18 ± 0.12	0.31 ± 0.11	0.39 ± 0.15
C$_9$H$_{17}$O$_7$S$^-$	269.0695	0.18 ± 0.23	0.06 ± 0.06	0.02 ± 0.01	0.09 ± 0.06
C$_{12}$H$_{23}$O$_5$S$^-$	279.1266	0.05 ± 0.04	0.03 ± 0.01	0.08 ± 0.06	0.11 ± 0.04
C$_9$H$_{17}$O$_4$S$^-$	221.0848	0.23 ± 0.39	0.57 ± 0.60	0.79 ± 0.46	1.20 ± 0.40
C$_9$H$_{17}$O$_6$S$^-$	253.0746	0.30 ± 0.32	0.21 ± 0.15	0.13 ± 0.06	0.31 ± 0.26
C$_{13}$H$_{25}$O$_5$S$^-$	293.1423	0.43 ± 0.32	0.26 ± 0.18	0.56 ± 0.32	0.88 ± 0.34
C$_{14}$H$_{27}$O$_5$S$^-$	307.1579	0.49 ± 0.31	0.32 ± 0.24	0.62 ± 0.41	0.88 ± 0.38
C$_{13}$H$_{25}$O$_6$S$^-$	309.1372	0.04 ± 0.04	0.04 ± 0.03	0.09 ± 0.07	0.16 ± 0.14
C$_{14}$H$_{27}$O$_6$S$^-$	323.1528	0.09 ± 0.08	0.13 ± 0.07	0.23 ± 0.21	0.43 ± 0.36
C$_{16}$H$_{31}$O$_5$S$^-$	335.1892	0.10 ± 0.11	0.17 ± 0.15	0.42 ± 0.43	0.44 ± 0.39
C$_{17}$H$_{33}$O$_5$S$^-$	363.2205	0.04 ± 0.01	0.23 ± 0.11	0.13 ± 0.10	0.16 ± 0.10
C$_{16}$H$_{31}$O$_6$S$^-$	351.1841	1.43 ± 0.92	2.64 ± 1.55	2.75 ± 2.39	4.87 ± 3.81
C$_{18}$H$_{35}$O$_5$S$^-$	363.2205	0.06 ± 0.06	0.06 ± 0.04	0.19 ± 0.19	0.31 ± 0.26
C$_{21}$H$_{41}$O$_5$S$^-$	405.2675	0.01 ± 0.01	0.01 ± 0.01	0.02 ± 0.03	0.02 ± 0.01
C$_8$H$_{15}$O$_5$S$^-$	223.0640	0.11 ± 0.05	0.18 ± 0.14	0.24 ± 0.10	0.29 ± 0.12
C$_7$H$_{13}$O$_6$S$^-$	225.0433	0.18 ± 0.18	0.12 ± 0.11	0.16 ± 0.16	0.30 ± 0.09
C$_8$H$_{15}$O$_6$S$^-$	239.0589	0.26 ± 0.17	0.54 ± 0.28	0.26 ± 0.10	0.46 ± 0.31
C$_{11}$H$_{21}$O$_5$S$^-$	265.1110	0.15 ± 0.06	0.14 ± 0.08	0.29 ± 0.14	0.49 ± 0.22
C$_{10}$H$_{19}$O$_6$S$^-$	267.0902	0.11 ± 0.08	0.12 ± 0.06	0.20 ± 0.08	0.21 ± 0.14
C$_7$H$_{13}$O$_9$S$^-$	273.0280	0.08 ± 0.07	0.30 ± 0.33	0.55 ± 0.29	0.38 ± 0.31
C$_{15}$H$_{29}$O$_5$S$^-$	321.1736	0.46 ± 0.40	0.27 ± 0.28	0.33 ± 0.38	0.47 ± 0.11
C$_{10}$H$_{17}$O$_6$S$^-$	265.0746	0.05 ± 0.02	0.06 ± 0.04	0.05 ± 0.03	0.11 ± 0.06
C$_9$H$_{15}$O$_5$S$^-$	235.0640	0.34 ± 0.24	0.41 ± 0.12	0.10 ± 0.06	0.15 ± 0.06
C$_{10}$H$_{17}$O$_5$S$^-$	249.0797	0.13 ± 0.07	0.55 ± 0.32	0.11 ± 0.04	0.28 ± 0.14
C$_9$H$_{15}$O$_6$S$^-$	251.0589	0.30 ± 0.29	0.19 ± 0.12	0.41 ± 0.27	0.43 ± 0.15
C$_{11}$H$_{19}$O$_6$S$^-$	279.0902	0.03 ± 0.02	0.03 ± 0.02	0.07 ± 0.04	0.10 ± 0.04
C$_8$H$_{13}$O$_6$S$^-$	237.0433	0.13 ± 0.06	0.09 ± 0.05	0.04 ± 0.01	0.08 ± 0.03
C$_9$H$_{15}$O$_7$S$^-$	267.0538	0.33 ± 0.39	0.10 ± 0.08	0.01 ± 0.01	0.05 ± 0.03
Aromatic OSs					
C$_9$H$_9$O$_4$S$^-$	213.0222	1.88 ± 1.62	0.91 ± 0.50	6.22 ± 3.54	18.88 ± 7.88
C$_6$H$_5$O$_4$S$^-$	172.9909	0.24 ± 0.08	0.27 ± 0.22	1.42 ± 1.02	0.72 ± 0.33
C$_7$H$_7$O$_4$S$^-$	187.0065	0.24 ± 0.18	0.25 ± 0.07	1.31 ± 0.55	0.56 ± 0.22
C$_{11}$H$_{19}$O$_{11}$S$^-$	359.0648	0.15 ± 0.05	0.16 ± 0.05	0.18 ± 0.07	0.38 ± 0.12
C$_{10}$H$_{17}$O$_{12}$S$^-$	361.0441	0.09 ± 0.01	0.11 ± 0.02	0.10 ± 0.01	0.10 ± 0.01
C$_7$H$_{11}$O$_{10}$S$^-$	287.0073	0.14 ± 0.05	0.14 ± 0.04	0.10 ± 0.02	0.12 ± 0.04
C$_8$H$_{13}$O$_9$S$^-$	285.0280	0.34 ± 0.24	0.23 ± 0.12	0.89 ± 0.75	0.44 ± 0.18
C$_8$H$_{13}$O$_{10}$S$^-$	301.0229	0.16 ± 0.08	0.15 ± 0.06	0.13 ± 0.04	0.17 ± 0.06
C$_{11}$H$_{17}$O$_{11}$S$^-$	357.0492	0.16 ± 0.16	0.21 ± 0.08	0.20 ± 0.10	0.12 ± 0.02
C$_9$H$_{11}$O$_{13}$S$^-$	358.9920	0.11 ± 0.03	0.12 ± 0.02	0.11 ± 0.02	0.12 ± 0.05
C$_8$H$_{12}$NO$_{11}$S$^-$	330.0131	0.20 ± 0.13	0.12 ± 0.03	0.14 ± 0.06	0.20 ± 0.12
C$_7$H$_7$SO$_4$S$^-$	218.9786	0.11 ± 0.04	0.14 ± 0.02	0.29 ± 0.08	0.19 ± 0.10

$C_8H_7O_5S^-$	215.0014	0.57 ± 0.30	0.33 ± 0.18	4.04 ± 3.58	1.77 ± 1.36
$C_8H_7NO_5S^-$	229.0045	0.61 ± 0.35	0.68 ± 0.41	0.87 ± 0.52	1.13 ± 0.47
$C_9H_9O_6S^-$	245.0120	0.29 ± 0.33	0.20 ± 0.06	0.70 ± 0.45	0.82 ± 0.41
$C_8H_7O_4S^-$	199.0065	0.73 ± 0.47	0.28 ± 0.13	2.51 ± 2.10	2.13 ± 0.79
$C_9H_7O_7S^-$	258.9912	0.54 ± 0.48	0.12 ± 0.03	0.35 ± 0.26	0.69 ± 1.34
$C_8H_5O_6S^-$	228.9807	0.38 ± 0.27	0.14 ± 0.03	0.58 ± 0.50	0.67 ± 0.91
$C_9H_7O_6S^-$	242.9963	0.48 ± 0.27	0.28 ± 0.13	1.61 ± 1.47	0.87 ± 0.73
$C_9H_3O_{11}S^-$	318.9396	0.08 ± 0.01	0.10 ± 0.01	0.09 ± 0.01	0.08 ± 0.00
$C_{10}H_5O_{12}S^-$	348.9502	0.08 ± 0.00	0.10 ± 0.01	0.08 ± 0.00	0.08 ± 0.01
$C_{34}H_{49}O_5S^-$	569.3301	0.11 ± 0.04	0.23 ± 0.20	0.57 ± 0.36	0.38 ± 0.26
$C_{43}H_{63}O_5S^-$	691.4396	0.33 ± 0.41	0.52 ± 0.34	0.11 ± 0.03	0.08 ± 0.01
$C_7H_{11}O_9S^-$	271.0124	0.27 ± 0.20	0.23 ± 0.12	0.17 ± 0.07	0.19 ± 0.08
$C_{10}H_7O_{11}S^-$	334.9709	0.08 ± 0.01	0.10 ± 0.01	0.08 ± 0.01	0.08 ± 0.01
$C_{10}H_5O_{11}S^-$	332.9553	0.08 ± 0.00	0.10 ± 0.01	0.09 ± 0.01	0.08 ± 0.00
$C_{10}H_5O_{10}S^-$	316.9603	0.07 ± 0.00	0.09 ± 0.01	0.08 ± 0.00	0.07 ± 0.00
$C_{12}H_7O_{13}S^-$	390.9607	0.08 ± 0.00	0.10 ± 0.01	0.08 ± 0.00	0.08 ± 0.00
$C_7H_5O_5S^-$	200.9858	0.84 ± 0.55	0.42 ± 0.36	3.18 ± 3.76	2.12 ± 2.18
$C_{18}H_{13}O_6S^-$	357.0433	0.11 ± 0.08	0.15 ± 0.05	0.13 ± 0.03	0.11 ± 0.02
$C_{23}H_{19}O_7S^-$	439.0851	0.22 ± 0.14	0.27 ± 0.15	0.14 ± 0.03	0.22 ± 0.11
$C_{25}H_{21}O_7S^-$	465.1008	0.08 ± 0.00	0.11 ± 0.02	0.08 ± 0.00	0.08 ± 0.00
$C_{24}H_{17}O_4S^-$	401.0848	0.38 ± 0.13	0.36 ± 0.14	0.40 ± 0.16	0.90 ± 0.25
$C_{27}H_{21}O_7S^-$	489.1008	0.11 ± 0.03	0.13 ± 0.04	0.10 ± 0.03	0.13 ± 0.03

162   [a]Aliphatic and aromatic OSs were generally considered as anthropogenic OSs (Riva et

163   al. 2016; Riva et al. 2015). All aliphatic and aromatic OSs and other anthropogenic

164   OSs were collectively referred to as anthropogenic OSs (OS_a).

165 **Table S4.** The mean mass concentrations of various OSs in PM$_{2.5}$ at different locations.

	Sampling site	Period	Season	OS$_i$ (ng m^{-3})	OS$_m$ (ng m^{-3})	C$_2$-C$_3$ (ng m^{-3})	OS$_a$ (ng m^{-3})	Total (ng m^{-3})	Ref.
Urban site	Atlanta, GA, USA	2014	Summer	1122.98	67.9	58.5	-	1249.38	(Hettiyadura et al. 2019a)
	Tianjing, China	2019	Winter	400.00	-	-	-	400.00	(Ding et al. 2022b)
	Lahore, Pakistan	2007	Winter	3.80	-	-	2.02	5.82	(Kundu et al. 2013)
	Hong Kong, China	2017	Winter	97.96	17.26	-	-	115.22	(Wang et al. 2022)
	Guangzhou, China	2017	Winter	88.03	20.96	-	-	108.99	
	Xian, China	2014	Winter	-	0.14	77.30	-	77.44	(Huang et al. 2018a)
	Shanghai, China	2021	Summer	85.38	30.61	19.31	23.38	158.68	(Yang et al. 2023)
	Urumqi, China	2018	Winter	62.21	23.33	41.85	168.54	295.93	(Yang et al. 2024)
Suburban site	Zion, Illinois, USA	2013	Spring	121.10	8.70	-		129.80	(Hughes et al. 2021)
Rural site	Look Rock, TN, USA	2013	Summer	1256.75	-	-	-	1256.75	(Budisulistiorini et al. 2015)
	Centreville,AL, USA	2013	Summer	15.40	-	20.83	1.16	37.39	(Hettiyadura et al. 2017)
	Yorkville, GA, USA	2010	Summer	115.11	-	-	-	115.11	(Lin et al. 2013)
	Copenhagen, Denmark	2011	Summer	11.31	0.87	-	-	12.18	(Nguyen et al. 2014)
	National Park, CO, USA	2016	Summer	19.00	-	-	-	-	(Chen et al. 2021)
	Seashore, CA, USA	2016	Summer	22.00	-	-	-	-	
Rural site	Melpitz, Germany	2013	Winter	11.12	49.33		32.83	93.28	(Glasius et al. 2018)
	Vavihill, Sweden	2013	Winter	2.75	6.39		4.15	13.29	
	Birkenes, Norway	2013	Winter	2.28	6.39		2.16	10.83	
Coastal site	The Yellow Sea and Bohai Sea	2019	Summer	22.98	7.53	12.7	-	43.21	(Wang et al. 2023)
Urban site	Guangzhou, China	2017	Winter	86.65	57.81	25.22	18.54	188.22	In this study

Kuming, China			61.12	58.9	28.55	18.22	166.79
Taiyuan, China			170.69	22.34	13.43	41.23	247.69
Xi'an, China			260.32	40.09	25.81	54.21	380.43

166 **Table S5.** The relative signal intensity of identified anthropogenic OSs in different
167 smoke particle samples. The relative signal intensity refers to the percentage of the
168 target OS signal intensity in the total signal intensity of the OS group to which it
169 belongs.

Formula [M-H]$^-$	Rice straw	Pine branch	Coal combustion	Gasoline vehicle	Diesel vehicle
Aliphatic OSs					
$C_8H_{17}O_4S^-$	2.91	0.09	11.23	1.62	0.86
$C_7H_{15}O_4S^-$	4.87	34.02	17.24	1.02	2.90
$C_9H_{19}O_4S^-$	2.92	3.27	2.57	3.81	1.21
$C_{10}H_{21}O_4S^-$	0.40	0.00	0.02	2.86	0.53
$C_9H_{17}O_4S^-$	3.80	0.09	7.35	7.59	59.32
$C_{14}H_{29}O_5S^-$	4.44	0.02	0.00	3.52	0.48
$C_7H_{15}O_5S^-$	0.98	1.02	2.08	0.30	0.47
$C_7H_{13}O_5S^-$	3.40	14.52	1.50	28.70	3.40
$C_9H_{17}O_5S^-$	1.76	3.55	1.27	0.48	0.59
$C_{10}H_{19}O_5S^-$	5.33	0.88	0.31	1.41	0.68
$C_{12}H_{23}O_5S^-$	0.66	1.22	0.02	1.34	1.72
$C_{13}H_{25}O_5S^-$	0.25	0.69	0.12	6.11	3.13
$C_{14}H_{27}O_5S^-$	0.29	2.12	0.00	0.70	0.64
$C_{16}H_{31}O_5S^-$	0.23	0.00	0.00	1.15	6.03
$C_{17}H_{33}O_5S^-$	16.49	7.62	0.17	0.68	0.49
$C_{18}H_{35}O_5S^-$	10.70	0.20	0.02	1.39	0.00
$C_{21}H_{41}O_5S^-$	3.44	0.01	0.02	0.20	0.00
$C_8H_{15}O_5S^-$	0.23	4.09	0.17	0.27	0.24
$C_{11}H_{21}O_5S^-$	0.07	0.48	0.05	0.62	0.28
$C_{15}H_{29}O_5S^-$	1.58	4.10	0.00	1.53	0.00
$C_9H_{15}O_5S^-$	0.68	2.59	0.82	1.98	1.69
$C_{10}H_{17}O_6S^-$	2.91	3.22	0.24	0.47	1.23
$C_9H_{17}O_6S^-$	1.77	2.84	0.11	0.98	0.72
$C_{13}H_{25}O_6S^-$	0.23	0.03	0.36	0.16	2.89
$C_{14}H_{27}O_6S^-$	0.17	0.00	0.24	1.08	5.60
$C_{16}H_{31}O_6S^-$	16.03	0.00	0.24	23.34	0.07
$C_7H_{13}O_6S^-$	0.35	2.65	0.08	0.41	0.21
$C_8H_{15}O_6S^-$	1.97	1.70	0.54	1.95	1.52
$C_{10}H_{19}O_6S^-$	3.47	0.97	47.71	0.44	1.00
$C_{10}H_{17}O_6S^-$	0.47	0.55	0.08	0.07	0.03
$C_9H_{15}O_6S^-$	0.16	1.20	0.33	1.08	0.93
$C_{11}H_{19}O_6S^-$	0.51	0.61	1.61	0.27	0.22
$C_{12}H_{21}O_6S^-$	0.10	0.00	0.00	0.02	0.03
$C_{14}H_{25}O_6S^-$	1.25	0.16	0.87	0.14	0.03
$C_8H_{13}O_6S^-$	0.51	0.89	1.41	0.87	0.28
$C_{12}H_{21}O_7S^-$	1.89	0.01	0.23	0.42	0.04
$C_9H_{17}O_7S^-$	2.18	0.47	0.69	0.36	0.33
$C_9H_{15}O_7S^-$	0.03	4.10	0.09	0.52	0.09
$C_7H_{13}O_9S^-$	0.43	0.03	0.16	0.04	0.06
$C_{26}H_{51}O_{12}S^-$	0.18	0.00	0.00	0.10	0.00
$C_{24}H_{51}N_2O_{13}S^-$	0.00	0.00	0.04	0.00	0.06

Aromatic OSs					
$C_{24}H_{17}O_4S^-$	4.88	0.21	0.08	28.12	9.48
$C_6H_5O_4S^-$	0.50	0.79	3.16	0.10	4.92
$C_7H_7O_4S^-$	1.65	0.95	12.12	1.37	14.60
$C_8H_7O_4S^-$	0.43	0.65	1.11	1.16	49.85
$C_9H_9O_4S^-$	75.53	25.38	71.45	1.80	86.58
$C_{34}H_{49}O_5S^-$	0.22	0.00	0.00	0.12	0.00
$C_{43}H_{63}O_5S^-$	0.05	0.22	0.00	0.00	0.17
$C_7H_5O_5S^-$	0.26	1.00	0.10	0.77	0.37
$C_8H_7NO_5S^-$	1.12	12.38	2.73	26.95	6.28
$C_8H_7O_5S^-$	1.67	2.04	2.32	0.86	9.55
$C_{18}H_{13}O_6S^-$	0.02	1.59	0.33	0.09	0.23
$C_8H_5O_6S^-$	0.25	0.09	0.15	0.11	0.83
$C_9H_7O_6S^-$	0.78	13.07	0.67	0.35	2.37
$C_9H_9O_6S^-$	1.67	5.31	0.86	0.39	6.95
$C_{23}H_{19}O_7S^-$	0.01	7.11	0.26	0.62	8.85
$C_{25}H_{21}O_7S^-$	0.02	0.10	0.01	0.09	0.01
$C_{27}H_{21}O_7S^-$	1.43	2.59	2.66	1.80	3.82
$C_9H_7O_7S^-$	0.06	0.09	0.02	0.12	0.70
$C_7H_{11}O_9S^-$	0.07	0.54	0.05	0.47	0.24
$C_8H_{13}O_9S^-$	0.94	4.31	0.26	0.60	0.77
$C_{10}H_5O_{10}S^-$	0.00	0.00	0.00	0.00	0.00
$C_7H_{11}O_{10}S^-$	0.00	0.37	0.00	0.09	0.01
$C_8H_{13}O_{10}S^-$	0.04	0.61	0.06	0.16	0.38
$C_{10}H_5O_{11}S^-$	0.00	0.09	0.01	0.00	0.00
$C_{10}H_7O_{11}S^-$	0.03	0.12	0.14	0.01	0.25
$C_{11}H_{17}O_{11}S^-$	0.18	1.68	0.38	0.70	2.71
$C_{11}H_{19}O_{11}S^-$	3.13	14.58	0.22	4.46	0.37
$C_{12}H_{21}N_2O_{11}S^-$	4.88	0.21	0.17	28.12	9.48
$C_8H_{12}NO_{11}S^-$	0.10	2.37	0.59	0.15	0.00
$C_9H_{13}O_{11}S^-$	0.06	1.55	0.04	0.17	0.84
$C_9H_3O_{11}S^-$	0.02	0.01	0.00	0.19	0.07
$C_{10}H_{17}O_{12}S^-$	0.00	0.00	0.07	0.01	0.07
$C_{10}H_5O_{12}S^-$	0.01	0.01	0.01	0.04	0.00

170
171

172 **Figure S1.**
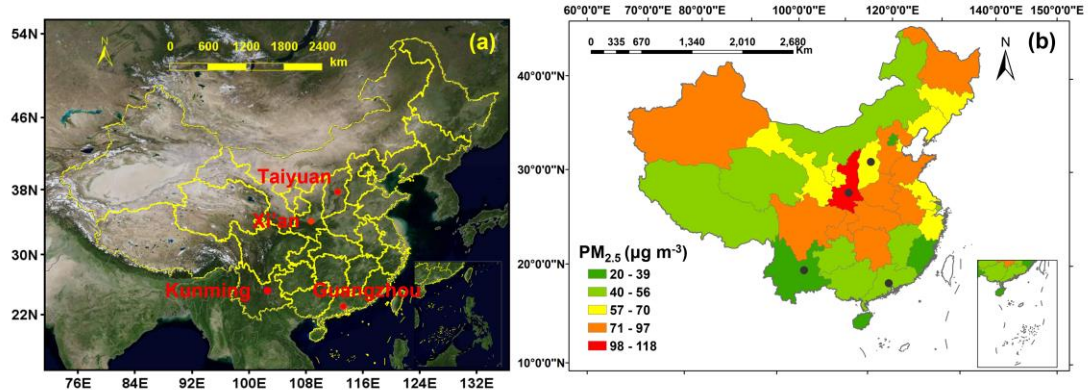
173

174 **Figure S1**. The locations of the sampling sites showing (a) the vegetation coverage in

175 China and (b) the PM$_{2.5}$ pollution situation during winter. The map was derived from

176 ©MeteoInfoMap (version 3.6.2) (Chinese Academy of Meteorological Sciences,

177 China).

178

179 **Figure S2.**

Figure S2. (a) Rice straw / Pine branches / Coal — Filter / Pump / Filter sampling. (b) Gasoline vehicle: Audi Q3, 95 octane gasoline / Diesel vehicle: R180 diesel engine — Filter sampling.
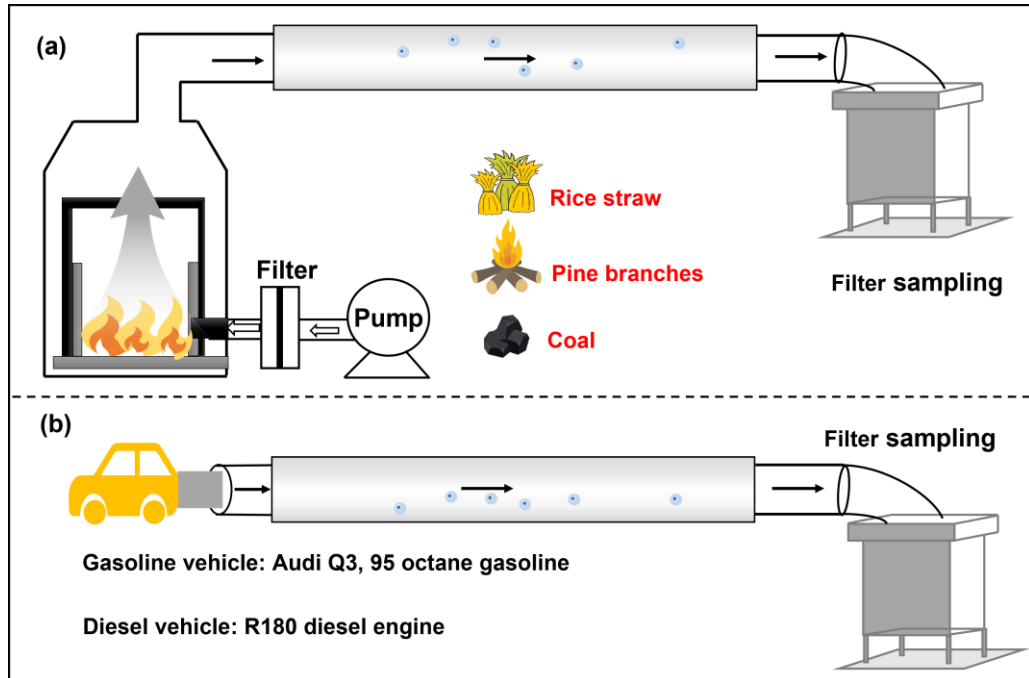
180

181 **Figure S2.** Schematic showing the collections of smoke particles derived from the

182 combustion of (a) rice straw, pine branches, and coal as well as from (b) liquid fuel

183 combustion (the gasoline vehicle was the Audi Q3, while the diesel vehicle features

184 the R180 diesel engine) (Tang et al. 2020). The samples were collected through a

185 combustion furnace pumped with filtered ambient air (particulate matter is removed).

186 **Figure S3.**
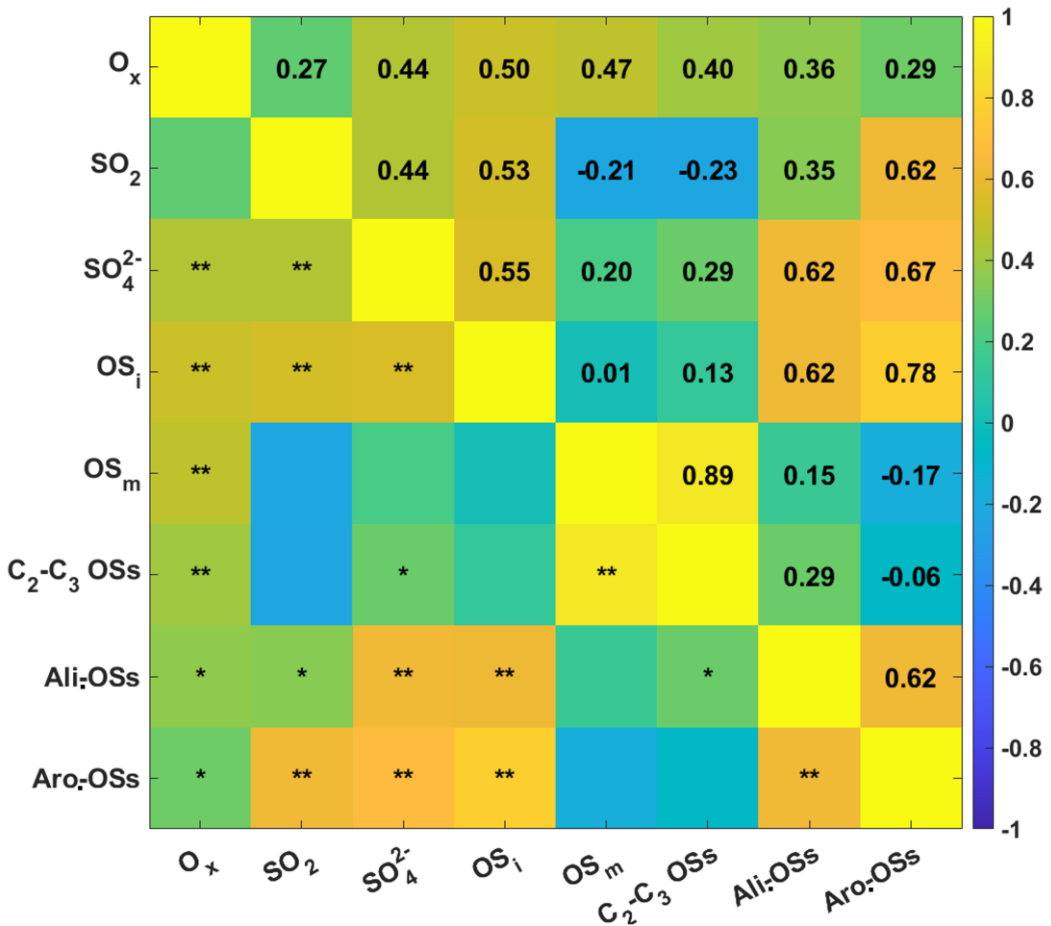
187

188 **Figure S3.** Diagrams presenting Pearson correlations among the concentrations of

189 OSs, O_x, SO_2, and SO_4^{2-}. The numbers in the matrix refer to the correlation

190 coefficients (r). Symbols * and ** indicate $P < 0.05$ and $P < 0.01$, respectively.

191

192

193   **Figure S4.**
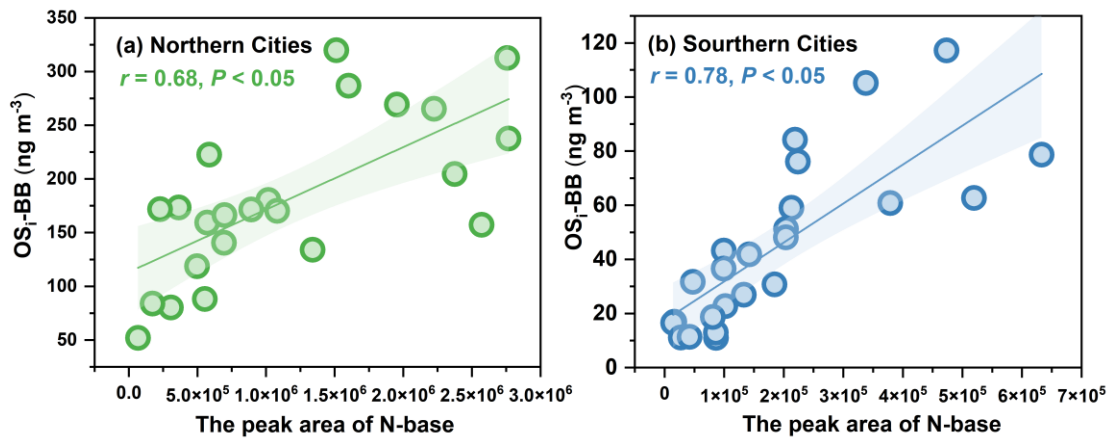
194

195   **Figure S4.** Mass concentrations of OS_i-BB (including $C_4H_7O_6S^-$, $C_5H_9O_6S^-$,

196    $C_5H_{11}O_6S^-$, $C_5H_7O_7S^-$, $C_4H_7O_5S^-$, $C_5H_{11}O_7S^-$, $C_5H_9O_7S^-$, and $C_5H_9O_8S^-$) as

197   functions of the abundances of N-base compounds (Wang et al. 2017c) for the cases in

198   (a) northern cities (b) southern cities.

199

200 **Figure S5.**

201
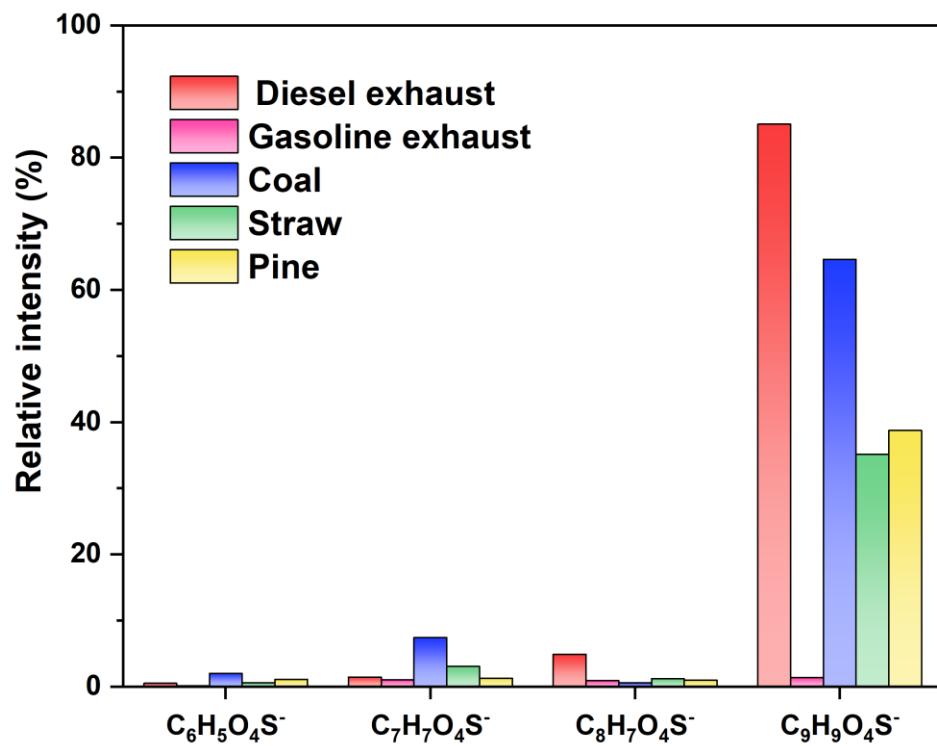
202 **Figure S5.** Mean relative signal intensities of typical aromatic OSs (i.e., $C_6H_5O_4S^-$,

203 $C_7H_7O_4S^-$, $C_8H_7O_4S^-$, and $C_9H_9O_4S^-$) in different smoke particle samples.

204

205

206   **Figure S6.**
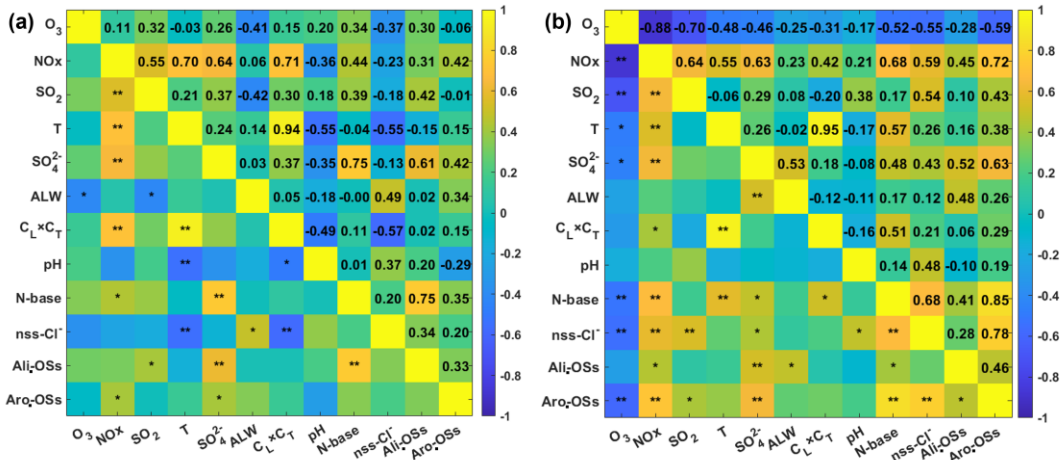
207

208   **Figure S6.** Diagrams presenting Pearson correlations among the different OS

209   subgroups and important parameters. The numbers in the matrix refer to the

210   correlation coefficients (*r*). Symbols * and ** indicate *P* < 0.05 and *P* < 0.01,

211   respectively.

212

213 **Figure S7.**
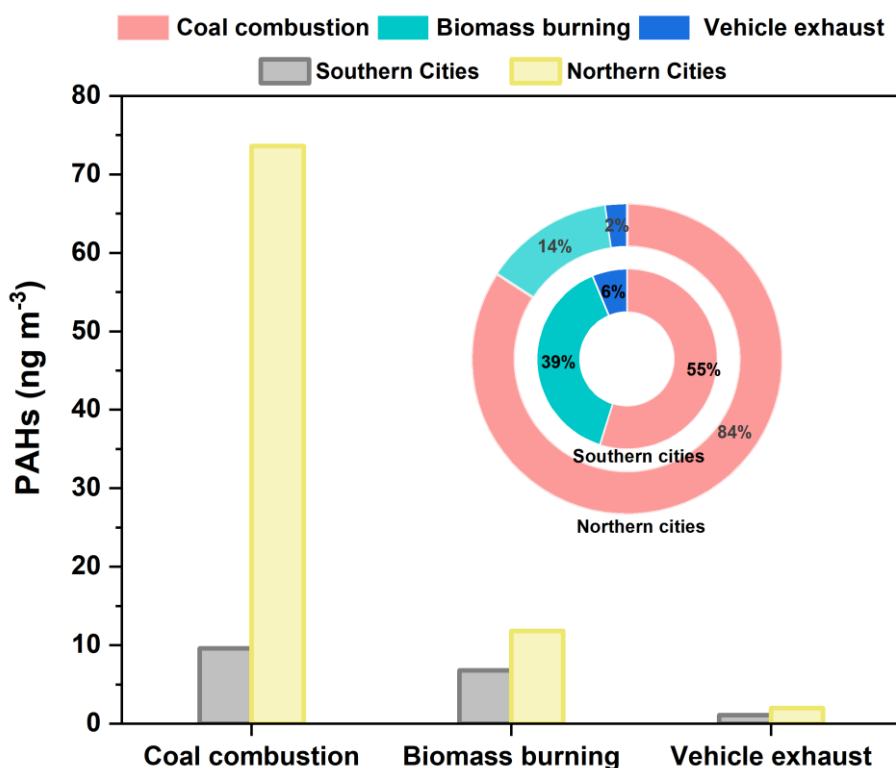
214

215 **Figure S7.** Variations in the concentration and percentage of polyaromatic

216 hydrocarbons (PAHs) emitted from coal combustion, biomass burning, and vehicle

217 exhaust in southern and northern cities. Data were derived from previous study (Yu et

218 al. 2020).

219

220 **Figure S8.**
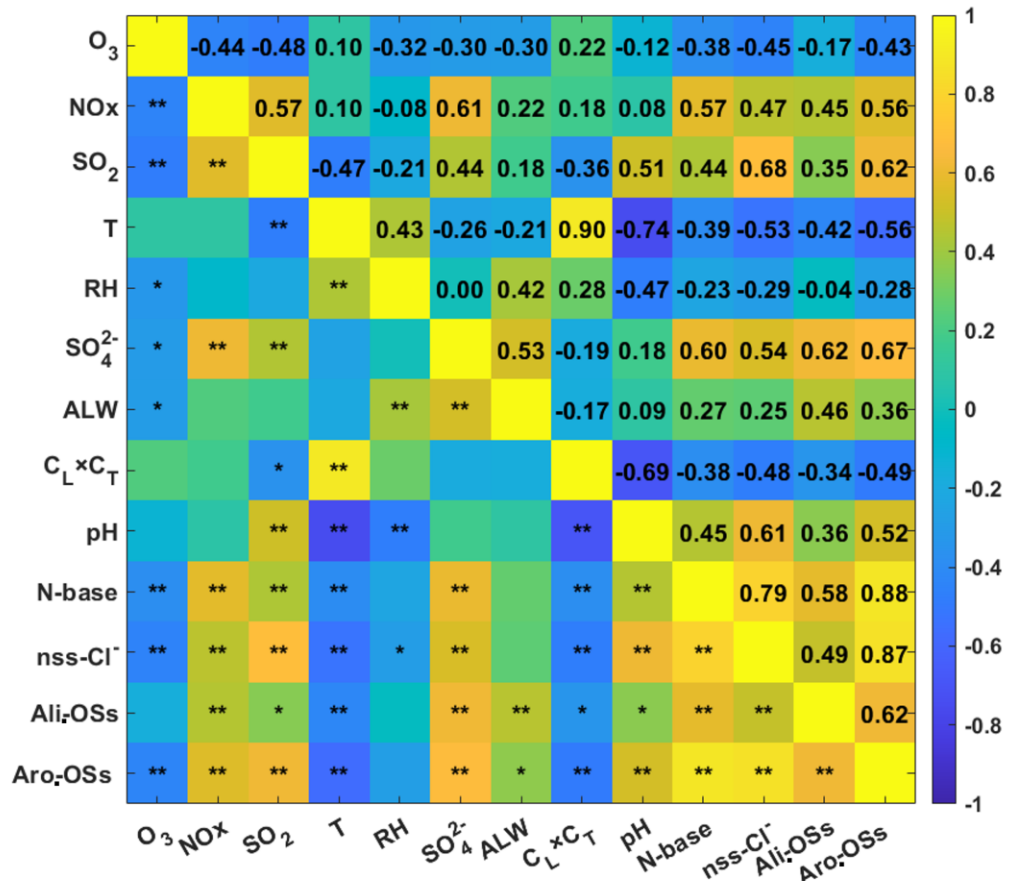
221

222 **Figure S8.** Diagrams presenting Pearson correlations among the different OS

223 subgroups and important parameters. The numbers in the matrix refer to the

224 correlation coefficients (*r*). Symbols * and ** indicate *P* < 0.05 and *P* < 0.01,

225 respectively.

226

227 **References**

228 Berndt, T., Mentler, B., Scholz, W., Fischer, L., Herrmann, H., Kulmala, M., and

229   Hansel, A.: Accretion Product Formation from Ozonolysis and OH Radical

230   Reaction of alpha-Pinene: Mechanistic Insight and the Influence of Isoprene

231   and Ethylene, Environ. Sci. Technol., 52, 11069-11077,

232   10.1021/acs.est.8b02210, 2018.

233 Berndt, T., Richters, S., Jokinen, T., Hyttinen, N., Kurten, T., Otkjaer, R. V.,

234   Kjaergaard, H. G., Stratmann, F., Herrmann, H., Sipila, M., Kulmala, M., and

235   Ehn, M.: Hydroxyl radical-induced formation of highly oxidized organic

236   compounds, Nat. Commun., 7, 13677, 10.1038/ncomms13677, 2016.

237 Boyd, C. M., Sanchez, J., Xu, L., Eugene, A. J., Nah, T., Tuet, W. Y., Guzman, M. I.,

238   and Ng, N. L.: Secondary organic aerosol formation from the β-pinene+NO3

239   system: effect of humidity and peroxy radical fate, Atmos. Chem. Phys., 15,

240   7497-7522, 10.5194/acp-15-7497-2015, 2015.

241 Bryant, D. J., Elzein, A., Newland, M., White, E., Swift, S., Watkins, A., Deng, W.,

242   Song, W., Wang, S., Zhang, Y., Wang, X., Rickard, A. R., and Hamilton, J. F.:

243   Importance of Oxidants and Temperature in the Formation of Biogenic

244   Organosulfates and Nitrooxy Organosulfates, ACS Earth and Space Chemistry,

245   5, 2291-2306, 10.1021/acsearthspacechem.1c00204, 2021.

246 Budisulistiorini, S. H., Li, X., Bairai, S. T., Renfro, J., Liu, Y., Liu, Y. J., McKinney, K.

247   A., Martin, S. T., McNeill, V. F., Pye, H. O. T., Nenes, A., Neff, M. E., Stone,

248   E. A., Mueller, S., Knote, C., Shaw, S. L., Zhang, Z., Gold, A., and Surratt, J.

249   D.: Examining the effects of anthropogenic emissions on isoprene-derived

250   secondary organic aerosol formation during the 2013 Southern Oxidant and

251   Aerosol Study (SOAS) at the Look Rock, Tennessee ground site, Atmos.

252   Chem. Phys., 15, 8871-8888, 10.5194/acp-15-8871-2015, 2015.

253 Cai, D., Wang, X., Chen, J., and Li, X.: Molecular Characterization of Organosulfates

254   in Highly Polluted Atmosphere Using Ultra-High-Resolution Mass

255   Spectrometry, J. Geophys. Res.Atmos., 125, 10.1029/2019jd032253, 2020.

256 Chen, Y., Dombek, T., Hand, J., Zhang, Z., Gold, A., Ault, A. P., Levine, K. E., and

257   Surratt, J. D.: Seasonal Contribution of Isoprene-Derived Organosulfates to

258   Total Water-Soluble Fine Particulate Organic Sulfur in the United States, ACS

259   Earth and Space Chemistry, 5, 2419-2432,

260   10.1021/acsearthspacechem.1c00102, 2021.

261 Ding, S., Chen, Y., Devineni, S. R., Pavuluri, C. M., and Li, X.-D.: Distribution

262   characteristics of organosulfates (OSs) in PM2.5 in Tianjin, Northern China:

263   Quantitative analysis of total and three OS species, Sci. Total Environ., 834,

264   10.1016/j.scitotenv.2022.155314, 2022a.

265 Ding, S., Chen, Y., Devineni, S. R., Pavuluri, C. M., and Li, X. D.: Distribution

266   characteristics of organosulfates (OSs) in PM2.5 in Tianjin, Northern China:

267   Quantitative analysis of total and three OS species, Sci. Total. Environ., 834,

268   155314, 10.1016/j.scitotenv.2022.155314, 2022b.

269 Ding, X., He, Q.-F., Shen, R.-Q., Yu, Q.-Q., Zhang, Y.-Q., Xin, J.-Y., Wen, T.-X., and

270   Wang, X.-M.: Spatial and seasonal variations of isoprene secondary organic

271   aerosol in China: Significant impact of biomass burning during winter,

272   Scientific Reports, 6, 10.1038/srep20411, 2016.

273 Ehn, M., Kleist, E., Junninen, H., Petäjä, T., Lönn, G., Schobesberger, S., Dal Maso,

274   M., Trimborn, A., Kulmala, M., Worsnop, D. R., Wahner, A., Wildt, J., and

275   Mentel, T. F.: Gas phase formation of extremely oxidized pinene reaction

276   products in chamber and ambient air, Atmos. Chem. Phys., 12, 5113-5127,

277   10.5194/acp-12-5113-2012, 2012.

278 Ehn, M., Thornton, J. A., Kleist, E., Sipila, M., Junninen, H., Pullinen, I., Springer, M.,

279   Rubach, F., Tillmann, R., Lee, B., Lopez-Hilfiker, F., Andres, S., Acir, I. H.,

280   Rissanen, M., Jokinen, T., Schobesberger, S., Kangasluoma, J., Kontkanen, J.,

281   Nieminen, T., Kurten, T., Nielsen, L. B., Jorgensen, S., Kjaergaard, H. G.,

282   Canagaratna, M., Maso, M. D., Berndt, T., Petaja, T., Wahner, A., Kerminen, V.

283   M., Kulmala, M., Worsnop, D. R., Wildt, J., and Mentel, T. F.: A large source

284   of low-volatility secondary organic aerosol, Nature, 506, 476-479,

285   10.1038/nature13032, 2014.

286 Glasius, M., Hansen, A. M. K., Claeys, M., Henzing, J. S., Jedynska, A. D., Kasper-

287   Giebl, A., Kistler, M., Kristensen, K., Martinsson, J., Maenhaut, W., Nøjgaard,

288   J. K., Spindler, G., Stenström, K. E., Swietlicki, E., Szidat, S., Simpson, D.,

289   and Yttri, K. E.: Composition and sources of carbonaceous aerosols in

290   Northern Europe during winter, Atmos. Environ., 173, 127-141,

291   10.1016/j.atmosenv.2017.11.005, 2018.

292 Guenther , A. B., Zimmerman, P. R., Harley, P. C., Monson, R. K., and Fall, R.:

Isoprene and monoterpene emission rate variability J. Geophys. Res.Atmos., 98, 12609-12617, 1993.

Guo, Y., Yan, C., Liu, Y., Qiao, X., Zheng, F., Zhang, Y., Zhou, Y., Li, C., Fan, X., Lin, Z., Feng, Z., Zhang, Y., Zheng, P., Tian, L., Nie, W., Wang, Z., Huang, D., Daellenbach, K. R., Yao, L., Dada, L., Bianchi, F., Jiang, J., Liu, Y., Kerminen, V.-M., and Kulmala, M.: Seasonal variation in oxygenated organic molecules in urban Beijing and their contribution to secondary organic aerosol, Atmos. Chem. Phys., 22, 10077-10097, 10.5194/acp-22-10077-2022, 2022.

Han, Y., Zhang, X., Li, L., Lin, Y., Zhu, C., Zhang, N., Wang, Q., and Cao, J.: Enhanced Production of Organosulfur Species during a Severe Winter Haze Episode in the Guanzhong Basin of Northwest China, Environ. Sci. Technol., 57, 8708-8718, 10.1021/acs.est.3c02914, 2023.

Hettiyadura, A. P. S., Al-Naiema, I. M., Hughes, D. D., Fang, T., and Stone, E. A.: Organosulfates in Atlanta, Georgia: anthropogenic influences on biogenic secondary organic aerosol formation, Atmos. Chem. Phys., 19, 3191-3206, 10.5194/acp-19-3191-2019, 2019a.

Hettiyadura, A. P. S., Al-Naiema, I. M., Hughes, D. D., Fang, T., and Stone, E. A.: Organosulfates in Atlanta, Georgia: anthropogenic influences on biogenic secondary organic aerosol formation, Atmos. Chem. Phys., 19, 3191-3206, 10.5194/acp-19-3191-2019, 2019b.

Hettiyadura, A. P. S., Stone, E. A., Kundu, S., Baker, Z., Geddes, E., Richards, K., and Humphry, T.: Determination of atmospheric organosulfates using HILIC

315   chromatography with MS detection, Atmos. Meas. Tech., 8, 2347-2358,

316   10.5194/amt-8-2347-2015, 2015.

317 Hettiyadura, A. P. S., Jayarathne, T., Baumann, K., Goldstein, A. H., de Gouw, J. A.,

318   Koss, A., Keutsch, F. N., Skog, K., and Stone, E. A.: Qualitative and

319   quantitative analysis of atmospheric organosulfates in Centreville, Alabama,

320   Atmos. Chem. Phys., 17, 1343-1359, 10.5194/acp-17-1343-2017, 2017.

321 Huang, L., Wang, Y., Zhao, Y., Hu, H., Yang, Y., Wang, Y., Yu, J. Z., Chen, T., Cheng,

322   Z., Li, C., Li, Z., and Xiao, H.: Biogenic and Anthropogenic Contributions to

323   Atmospheric Organosulfates in a Typical Megacity in Eastern China, J.

324   Geophys. Res.Atmos., 128, 10.1029/2023jd038848, 2023.

325 Huang, R.-J., Cao, J., Chen, Y., Yang, L., Shen, J., You, Q., Wang, K., Lin, C., Xu, W.,

326   Gao, B., Li, Y., Chen, Q., Hoffmann, T., O'Dowd, C. D., Bilde, M., and

327   Glasius, M.: Organosulfates in atmospheric aerosol: synthesis and quantitative

328   analysis of PM2:5 from Xi'an, northwestern China, Atoms. Meas. Tech., 11,

329   3447-3456, 10.5194/amt-11-3447-2018, 2018a.

330 Huang, R.-J., Cao, J., Chen, Y., Yang, L., Shen, J., You, Q., Wang, K., Lin, C., Xu, W.,

331   Gao, B., Li, Y., Chen, Q., Hoffmann, T., O'Dowd, C. D., Bilde, M., and

332   Glasius, M.: Organosulfates in atmospheric aerosol: synthesis and quantitative

333   analysis of PM2.5 from Xi'an, northwestern China, Atmos. Meas. Tech., 11,

334   3447-3456, 10.5194/amt-11-3447-2018, 2018b.

335 Hughes, D. D., Christiansen, M. B., Milani, A., Vermeuel, M. P., Novak, G. A., Alwe,

336   H. D., Dickens, A. F., Pierce, R. B., Millet, D. B., Bertram, T. H., Stanier, C.

337   O., and Stone, E. A.: PM2.5 chemistry, organosulfates, and secondary organic

338   aerosol during the 2017 Lake Michigan Ozone Study, Atmos. Environ., 244,

339   10.1016/j.atmosenv.2020.117939, 2021.

340 Jiang, H., Li, J., Tang, J., Cui, M., Zhao, S., Mo, Y., Tian, C., Zhang, X., Jiang, B.,

341   Liao, Y., Chen, Y., and Zhang, G.: Molecular characteristics, sources, and

342   formation pathways of organosulfur compounds in ambient aerosol in

343   Guangzhou, South China, Atmos. Chem. Phys., 22, 6919-6935, 10.5194/acp-

344   22-6919-2022, 2022.

345 Jokinen, T., Sipila, M., Richters, S., Kerminen, V. M., Paasonen, P., Stratmann, F.,

346   Worsnop, D., Kulmala, M., Ehn, M., Herrmann, H., and Berndt, T.: Rapid

347   autoxidation forms highly oxidized RO2 radicals in the atmosphere, Angew.

348   Chem. Int. Ed. Engl., 53, 14596-14600, 10.1002/anie.201408566, 2014.

349 Kundu, S., Quraishi, T. A., Yu, G., Suarez, C., Keutsch, F. N., and Stone, E. A.:

350   Evidence and quantitation of aromatic organosulfates in ambient aerosols in

351   Lahore, Pakistan, Atmos. Chem. Phys., 13, 4865-4875, 10.5194/acp-13-4865-

352   2013, 2013.

353 Lin, Y. H., Knipping, E. M., Edgerton, E. S., Shaw, S. L., and Surratt, J. D.:

354   Investigating the influences of SO2 and NH3 levels on isoprene-derived

355   secondary organic aerosol formation using conditional sampling approaches,

356   Atmos. Chem. Phys., 13, 8457-8470, 10.5194/acp-13-8457-2013, 2013.

357 Ma, J., Ungeheuer, F., Zheng, F., Du, W., Wang, Y., Cai, J., Zhou, Y., Yan, C., Liu, Y.,

358   Kulmala, M., Daellenbach, K. R., and Vogel, A. L.: Nontarget Screening

359   Exhibits a Seasonal Cycle of PM2.5 Organic Aerosol Composition in Beijing,

360   Environ. Sci. Technol., 56, 7017-7028, 10.1021/acs.est.1c06905, 2022.

361   Nguyen, Q. T., Christensen, M. K., Cozzi, F., Zare, A., Hansen, A. M. K., Kristensen,

362   K., Tulinius, T. E., Madsen, H. H., Christensen, J. H., Brandt, J., Massling, A.,

363   Nøjgaard, J. K., and Glasius, M.: Understanding the anthropogenic influence

364   on formation of biogenic secondary organic aerosols in Denmark via analysis

365   of organosulfates and related oxidation products, Atmos. Chem. Phys., 14,

366   8961-8981, 10.5194/acp-14-8961-2014, 2014.

367   Nozière, B., Ekström, S., Alsberg, T., and Holmström, S.: Radical-initiated formation

368   of organosulfates and surfactants in atmospheric aerosols, Geophys. Res. Lett.,

369   37, n/a-n/a, 10.1029/2009gl041683, 2010a.

370   Nozière, B., Ekström, S., Alsberg, T., and Holmström, S.: Radical-initiated formation

371   of organosulfates and surfactants in atmospheric aerosols, Geophys. Res. Lett.,

372   37, n/a-n/a, 10.1029/2009gl041683, 2010b.

373   Olson, C. N., Galloway, M. M., Yu, G., Hedman, C. J., Lockett, M. R., Yoon, T.,

374   Stone, E. A., Smith, L. M., and Keutsch, F. N.: Hydroxycarboxylic Acid-

375   Derived Organosulfates: Synthesis, Stability, and Quantification in Ambient

376   Aerosol, Environ. Sci. Technol., 45, 6468-6474, 10.1021/es201039p, 2011.

377   Riva, M., Budisulistiorini, S. H., Zhang, Z., Gold, A., and Surratt, J. D.: Chemical

378   characterization of secondary organic aerosol constituents from isoprene

379   ozonolysis in the presence of acidic aerosol, Atmos. Environ., 130, 5-13,

380   10.1016/j.atmosenv.2015.06.027, 2016.

381 Riva, M., Tomaz, S., Cui, T., Lin, Y. H., Perraudin, E., Gold, A., Stone, E. A.,

382   Villenave, E., and Surratt, J. D.: Evidence for an unrecognized secondary

383   anthropogenic source of organosulfates and sulfonates: gas-phase oxidation of

384   polycyclic aromatic hydrocarbons in the presence of sulfate aerosol, Environ.

385   Sci. Technol., 49, 6654-6664, 10.1021/acs.est.5b00836, 2015.

386 Surratt, J. D., Gómez-González, Y., Chan, A. W. H., Vermeylen, R., Shahgholi, M.,

387   Kleindienst, T. E., Edney, E. O., Offenberg, J. H., Lewandowski, M., Jaoui, M.,

388   Maenhaut, W., Claeys, M., Flagan, R. C., and Seinfeld, J. H.: Organosulfate

389   Formation in Biogenic Secondary Organic Aerosol, J. Phys. Chem. A., 112,

390   8345-8378, 10.1021/jp802310p, 2008.

391 Tang, J., Li, J., Su, T., Han, Y., Mo, Y., Jiang, H., Cui, M., Jiang, B., Chen, Y., Tang, J.,

392   Song, J., Peng, P. a., and Zhang, G.: Molecular compositions and optical

393   properties of dissolved brown carbon in biomass burning, coal combustion,

394   and vehicle emission aerosols illuminated by excitation–emission matrix

395   spectroscopy and Fourier transform ion cyclotron resonance mass

396   spectrometry analysis, Atmos. Chem. Phys., 20, 2513-2532, 10.5194/acp-20-

397   2513-2020, 2020.

398 Tao, S., Lu, X., Levac, N., Bateman, A. P., Nguyen, T. B., Bones, D. L., Nizkorodov,

399   S. A., Laskin, J., Laskin, A., and Yang, X.: Molecular characterization of

400   organosulfates in organic aerosols from Shanghai and Los Angeles urban areas

401   by nanospray-desorption electrospray ionization high-resolution mass

402   spectrometry, Environ. Sci. Technol., 48, 10993-11001, 10.1021/es5024674,

403   2014.

404   Trostl, J., Chuang, W. K., Gordon, H., Heinritzi, M., Yan, C., Molteni, U., Ahlm, L.,

405   Frege, C., Bianchi, F., Wagner, R., Simon, M., Lehtipalo, K., Williamson, C.,

406   Craven, J. S., Duplissy, J., Adamov, A., Almeida, J., Bernhammer, A. K.,

407   Breitenlechner, M., Brilke, S., Dias, A., Ehrhart, S., Flagan, R. C., Franchin,

408   A., Fuchs, C., Guida, R., Gysel, M., Hansel, A., Hoyle, C. R., Jokinen, T.,

409   Junninen, H., Kangasluoma, J., Keskinen, H., Kim, J., Krapf, M., Kurten, A.,

410   Laaksonen, A., Lawler, M., Leiminger, M., Mathot, S., Mohler, O., Nieminen,

411   T., Onnela, A., Petaja, T., Piel, F. M., Miettinen, P., Rissanen, M. P., Rondo, L.,

412   Sarnela, N., Schobesberger, S., Sengupta, K., Sipila, M., Smith, J. N., Steiner,

413   G., Tome, A., Virtanen, A., Wagner, A. C., Weingartner, E., Wimmer, D.,

414   Winkler, P. M., Ye, P., Carslaw, K. S., Curtius, J., Dommen, J., Kirkby, J.,

415   Kulmala, M., Riipinen, I., Worsnop, D. R., Donahue, N. M., and Baltensperger,

416   U.: The role of low-volatility organic compounds in initial particle growth in

417   the atmosphere, Nature, 533, 527-531, 10.1038/nature18271, 2016.

418   Wang, Y., Ren, J., Huang, X. H. H., Tong, R., and Yu, J. Z.: Synthesis of Four

419   Monoterpene-Derived   Organosulfates   and   Their   Quantification   in

420   Atmospheric   Aerosol   Samples,   Environ.   Sci.   Technol.,   51,   6791-6801,

421   10.1021/acs.est.7b01179, 2017a.

422   Wang, Y., Ren, J., Huang, X. H. H., Tong, R., and Yu, J. Z.: Synthesis of Four

423   Monoterpene-Derived   Organosulfates   and   Their   Quantification   in

424   Atmospheric   Aerosol   Samples,   Environ.   Sci.   Technol.,   51,   6791-6801,

425   10.1021/acs.est.7b01179, 2017b.

426 Wang, Y., Ma, Y., Kuang, B., Lin, P., Liang, Y., Huang, C., and Yu, J. Z.: Abundance

427   of organosulfates derived from biogenic volatile organic compounds: Seasonal

428   and spatial contrasts at four sites in China, Sci. Total Environ., 806,

429   10.1016/j.scitotenv.2021.151275, 2022.

430 Wang, Y., Zhao, Y., Wang, Y., Yu, J.-Z., Shao, J., Liu, P., Zhu, W., Cheng, Z., Li, Z.,

431   Yan, N., and Xiao, H.: Organosulfates in atmospheric aerosols in Shanghai,

432   China: seasonal and interannual variability, origin, and formation mechanisms,

433   Atmos. Chem. Phys., 21, 2959-2980, 10.5194/acp-21-2959-2021, 2021a.

434 Wang, Y., Hu, M., Wang, Y.-C., Li, X., Fang, X., Tang, R., Lu, S., Wu, Y., Guo, S., Wu,

435   Z., Hallquist, M., and Yu, J. Z.: Comparative Study of Particulate

436   Organosulfates in Contrasting Atmospheric Environments: Field Evidence for

437   the Significant Influence of Anthropogenic Sulfate and NOx, Environmental

438   Science & Technology Letters, 7, 787-794, 10.1021/acs.estlett.0c00550, 2020.

439 Wang, Y., Hu, M., Lin, P., Guo, Q., Wu, Z., Li, M., Zeng, L., Song, Y., Zeng, L., Wu,

440   Y., Guo, S., Huang, X., and He, L.: Molecular Characterization of Nitrogen-

441   Containing Organic Compounds in Humic-like Substances Emitted from

442   Straw Residue Burning, Environ. Sci. Technol., 51, 5951-5961,

443   10.1021/acs.est.7b00248, 2017c.

444 Wang, Y., Zhang, Y., Li, W., Wu, G., Qi, Y., Li, S., Zhu, W., Yu, J. Z., Yu, X., Zhang,

445   H.-H., Sun, J., Wang, W., Sheng, L., Yao, X., Gao, H., Huang, C., Ma, Y., and

446   Zhou, Y.: Important Roles and Formation of Atmospheric Organosulfates in

447   Marine Organic Aerosols: Influence of Phytoplankton Emissions and

448   Anthropogenic Pollutants, Environ. Sci. Technol., 57, 10284-10294,

449   10.1021/acs.est.3c01422, 2023.

450   Wang, Y., Hu, M., Guo, S., Wang, Y., Zheng, J., Yang, Y., Zhu, W., Tang, R., Li, X.,

451   Liu, Y., Le Breton, M., Du, Z., Shang, D., Wu, Y., Wu, Z., Song, Y., Lou, S.,

452   Hallquist, M., and Yu, J.: The secondary formation of organosulfates under

453   interactions between biogenic emissions and anthropogenic pollutants in

454   summer in Beijing, Atmos. Chem. Phys., 18, 10693-10713, 10.5194/acp-18-

455   10693-2018, 2018.

456   Wang, Z., Ehn, M., Rissanen, M. P., Garmash, O., Quéléver, L., Xing, L., Monge-

457   Palacios, M., Rantala, P., Donahue, N. M., Berndt, T., and Sarathy, S. M.:

458   Efficient alkane oxidation under combustion engine and atmospheric

459   conditions, Commun. Chem., 4, 10.1038/s42004-020-00445-3, 2021b.

460   Xie, Q., Su, S., Chen, J., Dai, Y., Yue, S., Su, H., Tong, H., Zhao, W., Ren, L., Xu, Y.,

461   Cao, D., Li, Y., Sun, Y., Wang, Z., Liu, C.-Q., Kawamura, K., Jiang, G., Cheng,

462   Y., and Fu, P.: Increase of nitrooxy organosulfates in firework-related urban

463   aerosols during Chinese New Year's Eve, Atmos. Chem. Phys., 21, 11453-

464   11465, 10.5194/acp-21-11453-2021, 2021.

465   Xie, Q., Li, Y., Yue, S., Su, S., Cao, D., Xu, Y., Chen, J., Tong, H., Su, H., Cheng, Y.,

466   Zhao, W., Hu, W., Wang, Z., Yang, T., Pan, X., Sun, Y., Wang, Z., Liu, C. Q.,

467   Kawamura, K., Jiang, G., Shiraiwa, M., and Fu, P.: Increase of High

468   Molecular Weight Organosulfate With Intensifying Urban Air Pollution in the

469   Megacity Beijing, J. Geophys. Res.: Atmos. , 125, 10.1029/2019jd032200,

470   2020.

471   Yan, C., Nie, W., Äijälä, M., Rissanen, M. P., Canagaratna, M. R., Massoli, P.,

472   Junninen, H., Jokinen, T., Sarnela, N., Häme, S. A. K., Schobesberger, S.,

473   Canonaco, F., Yao, L., Prévôt, A. S. H., Petäjä, T., Kulmala, M., Sipilä, M.,

474   Worsnop, D. R., and Ehn, M.: Source characterization of highly oxidized

475   multifunctional compounds in a boreal forest environment using positive

476   matrix factorization, Atmos. Chem. Phys., 16, 12715-12731, 10.5194/acp-16-

477   12715-2016, 2016.

478   Yang, T., Xu, Y., Ma, Y.-J., Wang, Y.-C., Yu, J. Z., Sun, Q.-B., Xiao, H.-W., Xiao, H.-

479   Y., and Liu, C.-Q.: Field Evidence for Constraints of Nearly Dry and Weakly

480   Acidic Aerosol Conditions on the Formation of Organosulfates,

481   Environmental Science & Technology Letters, 10.1021/acs.estlett.4c00522,

482   2024.

483   Yang, T., Xu, Y., Ye, Q., Ma, Y.-J., Wang, Y.-C., Yu, J.-Z., Duan, Y.-S., Li, C.-X., Xiao,

484   H.-W., Li, Z.-Y., Zhao, Y., and Xiao, H.-Y.: Spatial and diurnal variations of

485   aerosol organosulfates in summertime Shanghai, China: potential influence of

486   photochemical processes and anthropogenic sulfate pollution, Atmos. Chem.

487   Phys., 23, 13433-13450, 10.5194/acp-23-13433-2023, 2023.

488   Yassine, M. M., Dabek-Zlotorzynska, E., Harir, M., and Schmitt-Kopplin, P.:

489   Identification of weak and strong organic acids in atmospheric aerosols by

490   capillary electrophoresis/mass spectrometry and ultra-high-resolution Fourier

491   transform ion cyclotron resonance mass spectrometry, Anal. Chem., 84, 6586-

492   6594, 10.1021/ac300798g, 2012.

493   Yassine, M. M., Harir, M., Dabek-Zlotorzynska, E., and Schmitt-Kopplin, P.:

494   Structural characterization of organic aerosol using Fourier transform ion

495   cyclotron resonance mass spectrometry: aromaticity equivalent approach,

496   Rapid. Commun. Mass. Spectrom., 28, 2445-2454, 10.1002/rcm.7038, 2014.

497   Ye, Y., Zhan, H., Yu, X., Li, J., Wang, X., and Xie, Z.: Detection of organosulfates and

498   nitrooxy-organosulfates in Arctic and Antarctic atmospheric aerosols, using

499   ultra-high resolution FT-ICR mass spectrometry, Sci. Total Environ., 767,

500   10.1016/j.scitotenv.2020.144339, 2021.

501   Yu, Q., Ding, X., He, Q., Yang, W., Zhu, M., Li, S., Zhang, R., Shen, R., Zhang, Y., Bi,

502   X., Wang, Y., Peng, P. a., and Wang, X.: Nationwide increase of polycyclic

503   aromatic hydrocarbons in ultrafine particles during winter over China revealed

504   by size-segregated measurements, Atmos. Chem. Phys., 20, 14581-14595,

505   10.5194/acp-20-14581-2020, 2020.

506